LAWRENCE
LIVERMORE
NATIONAL
LABORATORY

UCRL-TR-227708

Development of Technologies to Utilize Laser Plasma Radiations Sources for Radiation Effects Sciences

J. F. Davis

February 2, 2007

This work was performed under the auspices of the U.S. Department of Energy by University of California, Lawrence Livermore National Laboratory under Contract W-7405-Eng-48.

Final Report
Contract B555289

Development of Technologies to Utilize Laser Plasma Radiations Sources for Radiation Effects Sciences

December 2006

Prepared by:
John F. Davis
Alme & Associates

Prepared for:
Kevin B. Fournier
Lawrence Livermore National Laboratory
4000 Avenue East, L-473
Livermore, CA 94550

Final Report
Contract B555289
Development of Technologies to Utilize Laser Plasma Radiations Sources for Radiation Effects Sciences

I. Introduction

This final report will cover work performed over the period of November 11, 2005 to September 30, 2006 on the contract to develop technologies using laser sources for radiation effects sciences. The report will discuss four topic areas; the laser source experiments on the Gekko Laser at Osaka, Japan, planning for the Charge State Freeze Out experiments to be performed in calendar year 2007, a review of previous xenon gasbags on the LANL Trident laser to provide planning support to the May-June 2007 HELEN experiments.

II. Gekko

Notes on the joint Japanese, LLNL and CEA experiments held March 2006 on the GEKKO XII laser at ILE, Osaka, Japan. The initial objectives of the experiment were;

1) A comparison between the Ti-doped SiO_2 aerogel material of LLNL and the Ti-doped plastic foam of ILE.
2) Study the effect on (a) X-ray yield and (b) laser-heat-front propagation of preheating the targets with a 2T laser prepulse.
3) To obtain time-dependent spectroscopy of the Ti K-shell emission
4) Cross-calibration among LLNL x-ray photo-diode (XPD), CEA XPD, and ILE X-ray crystal spectrograph with CCD.

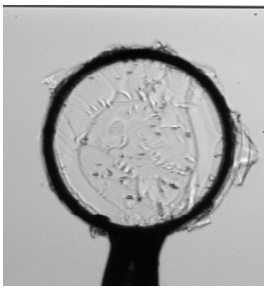

Fig. 1 Doped aerogel in Be cylinder (LLNL).

For the laser, there were nine "drive" beams at 3ω, with pulse durations τ = 2.5ns, and 200 J/beam (1.8 kJ in total), while for the three "foot" beams at 2ω, τ = 2.0ns, with 100 J/beam. The intensity profile of the drive beams is smoothed by SSD while the foot beams are smoothed by the method of partially coherent light.

Unfortunately, problems with target fabrication forced changes in the shot matrix and the experiment objectives. The final targets were Ti-doped SiO_2 aerogels in glass tubes, Ti foils and the Ge-doped aerogels. The final shot matrix focused on effects of laser focusing and alignment conditions on the x-ray yield and target performance.

The XRD array was an eight-channel bi-planar vacuum diode array that was mounted on a standard-sized vacuum flange, which is an integral part of the unit. The diode cathodes are aluminum surfaces that have been dry machined to an ultra smooth surface with a diameter of 0.635 cm. Each of the cathodes is enclosed in its own anode cavity consisting of a cylindrical cap covered with a thin 90% transparent nickel mesh. The entire unit was enclosed by an aluminum cylindrical block with holes above each detector channel for the filters. The bias on the XRDs was (typically) –200V with each channel independently biased via the NRL built bias

box. The gain of the XRDs is not dependent on the bias voltage supplied. The XRDs were mounted directly on the GEKKO XII vacuum tank and the distance from the TCC to the XRDs was 111 cm.

Table 1, below shows the filters used for the 8 channels of the XRD array. Note that over all channels was a 12.5 micron beryllium foil and one layer of 5 micron nickel mesh (2000 holes per inch) with a transmission of 62%. The observed signals were evaluated by a NRL developed IDL code which deconvolves the best spectral fit to the observed signals using as input the response functions of each of the filtered XRDs, the distance to TCC, and incident laser energy. Output is assumed to isotropic into four pi. Key to successful deconvolution is a reasonably accurate start spectrum with the line features of the observed spectrum. Figures 3 & 4 attached show the spectral response functions of the filtered XRDs and the start spectrum for Ti doped SiO_2 aerogel targets.

Table 1: XRD array used at Gekko*

Channel	Filter	K-edge	thickness (microns)
1	Si	1.838	22.15
2	Saran (Cl)	2.815	38.1
3	Ti	4.965	22.0
4	V	5.47	25.86
5	Fe	7.12	10.0
6	Co	7.709	8.5
7	Ni	8.33	10.0
8	Cu	8.979	10.0

*Note that there was 12.5um Be overall and 1 layer of 5 micron Ni mesh with a transmission of 62%.

For the January 2007 GEKKO campaign, the possible targets are; higher concentration Ti in SiO_2 aerogel contained in beryllium cylinders, pure Ti oxide, Ti-coated nanowires, iron "smoke" targets and Tin (Sn) nanowires.

Table 2: Possible spectral emission from new targets for GEKKO campaign 2007

Element	Z	Emission region	
Sn	Z= 50 L-edge at 3.929	L-shell emission at ~3.9 – 4.5	
Ti	Z= 22 K-edge at 4.965 *Ti Kα below Ti K-edge	Heα at 4.75 keV Heβ at 5.58 keV	L-shell few hundred eV
Fe	Z= 26 K-edge at 7.112 *Fe Kα below Fe K-edge	Lyα at 6.952 keV	L-shell below 1 keV

For the GEKKO 2007 experimental campaign it is suggested to change out one, maybe two of the higher energy filtered XRD channels for filters with edges below the Ti K-edge at 4.965 keV. Possible alternate filters include;

Filter	K-edge	thickness (microns)	note
Mg	1.305 keV	15 μm	CEA uses 15μm
Zr	2.23 keV	4-5 μm	CEA uses 5μm Zr
Mo	2.52 keV		
	L-edge		
Ag	3.35 keV	3-4 μm	CEA uses 5μm Ag
Sn	3.929	6-7 μm	

III. Charge State Freeze Out

The overall objective of the charge state freeze out experiments (CSFO) is to develop an experimental/calculational campaign to understand expansion of hot, dense matter into vacuum and to obtain experimental data to verify the code predictions. The near term experimental objective is to develop an experiment to uniformly heat known material (low-Z) to temperatures to provide formation of multiple ionization states (of order 2-5+) and allow the plasma to expand and observe charge states as function of time and density. The initial experiments will be with a low-Z target for example, SiO_2. This will limit the range of ionization states present and may allow optical spectroscopic techniques to be applied for T_e, n_e, and other plasma parameters. Also, low Z materials will have a lot simpler spectrum in comparison to higher Z materials.

The objective here is to estimate the experimental conditions to be expected as the laser heated low density material expands into a vacuum. Estimates will be made of the evolution of the plasma and the expected ion flux at diagnostics. An estimate of when in the expansion will the ion charge state be 'frozen out' and what will that charge state will be attempted. Assume at time $t = t_o$ that a laser heats a low density material to an initial temperature T_o and it has not moved and the density and temperature are a constant throughout ($T_e = T_i$). It is assumed that the initial temperatures will be order 10-100 eV and mass densities of order 1-5 mg/cm^3. It is also assumed that the expansion will be isotropic.

Ion Expansion Velocities

With these assumptions on initial conditions, what do we expect to happen. The hot material at the outer edge will expand into the vacuum at a maximum expansion velocity of a hot material given by:

$$v_{exp} = [2/((-1)]^{1/2} * c_s$$

where γ is the ratio of specific heats and c_s is the ion sound speed given by

$$c_s = [(RZT/A]^{1/2}$$

Note that the ion sound speed is proportional to the square root of the ion charge state. Coincident with the outer material expansion, a rarification wave will propagate into the hot

material at the ion sound speed. As the rarification wave propagates, then at the sonic interface, the hot material will then expand out at the expansion velocity. Assuming that the temperature remains constant during the time for the rarification wave to reach the center of the target identifies a characteristic time for the target to expand and then to move radially with a common expansion velocity. This time is

$$\tau_{ch} = r_o/c_s$$

and a characteristic scale length of

$$l \approx r_o + v_{exp}\,\tau_{ch} = r_o(1 + v_{exp}/c_s), \text{ which is just } r_o[1 + (2/(\gamma\text{-}1))^{1/2}].$$

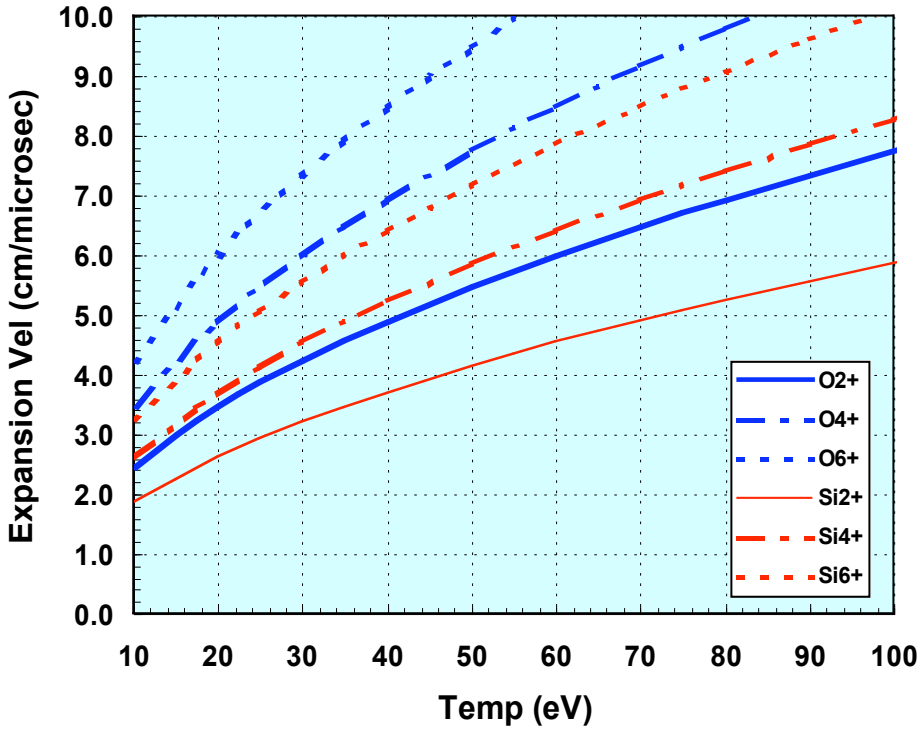

Figure 3: Calculated expansion velocities of silicon and oxygen ions versus temperature and charge state.

For a 200 micron radius target and an initial temperature of 50 eV for a SiO_2 aerogel this gives a sound velocity of the Si^{4+} ions of order 6 cm/μs and thus the characteristic time and scale length are:

$$\tau_{ch} = r_o/c_s \approx 3.3 \text{ ns} \quad \text{and} \quad l \approx 550 \text{ microns}$$

<u>Electron-Ion and Electron-Electron Collisions</u>
Note the electron-ion thermal equilibration time is given by

$$\tau_{e/i} = 1/\nu^{e/i} = 3.125\text{x}10^{8}\ A\ T_e^{3/2}\ (n_i\ Z^3\ \ln\Lambda)^{-1}\ \ \text{sec}$$

Again for an initial temperature of 50 eV in our SiO_2 aerogel we can estimate the initial degree of ionization and electron density. Noting that for a plasma in LTE, the degree of ionization is approximately 2-3X the electron temperature. Thus, referring the table of Si and O ionization energies, for an initial temperature of 50 eV we would expect $Z \approx 4\text{-}5$. The coulomb logarithm is of order 4.5 and with $n_e = Zn_i$ where n_i is given by (note that at temperatures of interest $n_o = 0$);

$$n_i = \{m\ (g/cc) \bullet Avo \bullet \#atoms/molecule\} / A'(molecular\ wt)$$

For our case of SiO_2, m = 1-3 mg/cc, $A' = 60$ and

$$n_i = 3\text{-}9\text{x}10^{19}\ ions/cm^3$$

Note that $r_o = 200$ microns, and the volume = $4/3\ \pi\ r_o^3 = 3.35\text{x}10^{-5}\ cm^3$
and therefore the total number of ions is;

$$N_i = 1\text{-}3\text{x}10^{15}\ atoms$$

substituting the initial electron-ion thermal equilibration time will be

$1/\nu^{e/i} \approx 540$ psec for the lower density case.

Table III: Si and O ionization energies

Silicon	eV	Oxygen	eV
Si I	8.15	O I	13.618
Si II	16.35	O II	35.184
Si III	33.49	O III	54.93
Si IV	45.14	O IV	77.52
Si V	166.77	O V	113.90
Si VI	205.27	O VI	138.11
Si VII	246.50	O VII	739.30
Si VIII	303.54	O VIII	871.00
Si IX	351.13		
Si X	401.38		
Si XI	476.36		
Si XII	523.43		
Si XIII	2,427.65		
Si IV	2,673.20		

The electron-electron collision frequency will be very high, initially thermalization times ($1/\nu^{e/e}$) of order 0.1 ps, and will remain high during the initial plasma expansion. The electron-electron thermalization times will still $\nu_e \sim 1$ ns when the plasma density is down 5-6 orders of magnitude.

This would imply that during the initial expansion that the electrons will remain coupled to the interior of the unexpanded plasma, and will be cooling due to volumetric cooling. The ions that are expanding into the vacuum will rapidly cool and be disconnected collisionally soon after the passage of the rarification wave.

Post Heating, Early Time Plasma Conditions

Thus it might be reasonable to assume that as long as the electron-electron collision frequency is high, there will be a relatively uniform temperature in the hot material, and this would be across the sonic interface. This would continue until the collision frequency of the electrons is not adequate to maintain LTE. Thus it is then reasonable to assume isotropic expansion and a perfect gas

$$T/T_o = V_o/V \qquad \Rightarrow \qquad T/T_o(@\, t = \tau_{ch}) = [1 + (2/(\gamma\text{-}1))^{1/2}]^{-3}$$

$$T/T_o(@\, t = \tau_{ch}) = (2.728)^{-3} = 0.0493 \approx 1/20$$

Remembering that the characteristic timescale is

$$\tau_{ch} = r_o/c_s \approx 3.3 \text{ ns} \quad \text{and} \quad l \approx 550 \text{ microns}$$

Thus, on the time scale of order 3 nanoseconds, the initial target has a 20X change in volume and a corresponding decrease in temperature (T_e) of 1/20. For an initial T_e of 50 eV, implies that the T_e decreases to order of 2.5 eV in about 3-6 nanoseconds. Noting from above the electron-ion thermalization time even at t_o the thermalization time will be long relative to the rate of change of the electron temperature due to the expansion. However, the plasma in the interior will be at the initial high density until the rarification wave arrives, thus the ions will continue to be somewhat collisionally connected to the electrons (quasi-LTE).

However, also note that in the characteristic timescale the rarification wave speed in the target material would decrease $\approx\sqrt{20}$ or about 4.5X. Thus, as the outer material expands at an expansion velocity given by the initial (assumed uniform) temperature, the material in the interior would not have moved, but T_e would have decreased as a function of the expanding volume (remembering that the interior is coupled to the expanding plasma by the high electron collision frequency), cooling the interior ions by electron-ion collisions. Thus when the rarification wave arrives the material will expand at a much reduced velocity. But note that the local ion sound speed will be dependent on a) the reduced ion temperature that is dependent on the electron-ion thermalization times, and b) on the reduced ion charge state due to recombination. The sound speed at the sonic interface will lag behind the electron temperature due to the much longer long ion-electron thermalization timescales, and it is expected that in the interior of the plasma, $T_i > T_e$. Thus an estimated timescale for the rarification wave to reach the center of the target (for a 200 micron diameter target) is ~10 ns.

So, on a time scale of order (for our example) ~10 ns all the target will be expanding radially but with a distribution of velocities. Thus, at our detector system, we would expect to see a distribution of plasma velocities arriving with the exterior material arriving at velocities characteristic of the initial temperature (highest velocities) and the interior material having

velocities determined by collisional and radiative process in the first few nanoseconds of the expansion.

Radiation and Recombination

Of course things are not so simple. We must also look at radiation and recombination. Assuming a blackbody emitter;

$$P_{rad} = \sigma T^4 \bullet \text{Area or} \quad P_{rad} \approx 6.44\text{x}10^{11}\, T^4 \bullet \text{Area} \quad \text{eV/ps-cm}^2$$

For a 200 micron diameter sphere and 50 eV

$$P_{rad} \approx 2\text{x}10^{16} \text{ eV/picosecond}$$

which is about ½ of the total thermal energy in the sphere. This of course is non-physical as the radiation rate will not only be tied to T_e, but also to T_i, to the radiative recombination rates, and to the atomic spontaneous emission rates of the exited species. As shown, the thermal relaxation time between the electrons and ions is of order 500 picoseconds and increasing rapidly as the plasma expands and cools. The spontaneous emission rates for Si IV or V are typically of order a few ps to 100's ps. Thus we would expect the exterior of the plasma sphere to cool rapidly due to the expansion and to radiation cooling. The electron temperature will remain coupled to the bulk plasma sphere and we would therefore expect high thermal gradients that will complicate the expansion process due to rapidly changing recombination and collision rates towards the interior of the plasma. The high electron collision frequency will continue to dominate the populations of the excited states and we would expect LTE in the interior of the plasma. As the plasma expands radially outward from the sphere, it becomes optically thin (and cold) on nanosecond timescales. Thus, we would expect that the radiating surface will be at or near the sonic interface and the expanding cooler plasma will not be in LTE.

Let's take a quick look at recombination. The local recombination rates of the plasma will be given by:

$$dn_e/dt = n_e - \alpha_1 n_e n_i - \alpha_2 n_e^2 n_i$$

where α_1 is the radiation recombination rate

$$\alpha_1 \approx 2.7\text{x}10^{-13}\, Z^2\, T_e^{-0.5} \text{ cm}^3/\text{s}$$

and α_2 is the two-body recombination rate

$$\alpha_2 \approx 8.77\text{x}10^{-27}\, Z^2\, T_e^{-4.5} \text{ cm}^6/\text{s}$$

Note that both rates are dependent on T_e and will increase as T_e decreases. If we take a simplified look assuming that T_e can be approximated by assuming isotropic expansion of the bulk plasma and that n_i is a function of the recombination rate and to the bulk expansion, we can get a first look at the change in n_e, n_i and Z in the first few nanoseconds after laser heating.

Assume initial conditions of ;
T_e = 50 eV
n_i = $9x10^{19}$ /cm^3
Z = 4.5

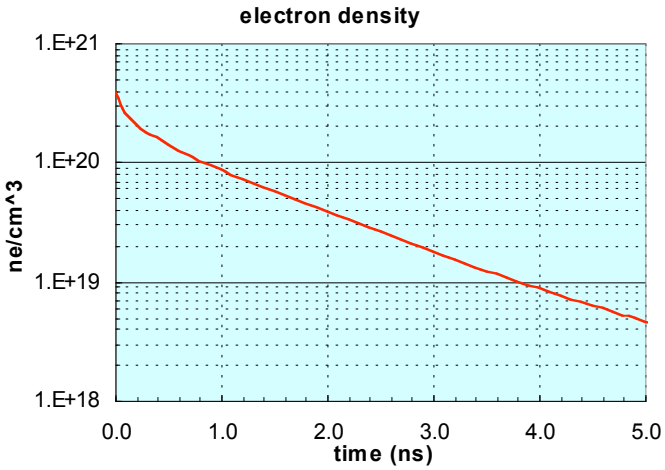

Thus, on our characteristic timescale (5 ns), the electron density would decrease two orders of magnitude. Note that we have not included radiation cooling which will increase the cooling rate, increasing the local recombination rate. This means that initially the plasma will expand at velocities characteristic of the initial T_e and with the degree of ionization near that of t_o. But in timescales much shorter than our characteristic timescale (e.g. ~ 1 ns), the average ionization level will have gone from Z ≈ 4.5 to Z ≈ 2 and T_e would have decreased about factor of 2 or more.

Debye Lengths

The primary objective of the experiment is to measure the charge state distribution of the free expanding plasma. As shown, the higher charge state ions will typically have higher temperatures before expansion and therefore are expected to arrive at a ion detector system first. Also, we can conclude that the ion plasma that subsequently arrives at the detector system will have a distribution of charge states. Thus, the ion detector system must distinguish the charge state of the ion upon arrival. This is to be accomplished by a detector system using magnetic and/or electric fields to bend the ions dependent on their charge state (and velocity). Within the detector system it is necessary to have only the ions to the detector plane. The arriving plasma will be charge neutral so the plasma electrons need to be stripped off upon entrance to the ion detector system by using a grounded or perhaps biased pinhole or slit.

The size of the pinhole or slit must be smaller than the plasma debye length.

$$\lambda_D = 743 \sqrt{T_e/n_e} \quad \text{cm}$$

At ~ 5ns the electron density is of order $3x10^{18}$ /cm^3 and T_e ~ 6 eV (in the expansion cloud) thus at this time

$\lambda_D \approx$ 0.01 microns.

But as shown previously, on timescales of order 10 ns we would expect all of the target material to be moving radially with the outer material (for our example of I_{nitial} = 50 eV) at velocities ≈ 6 cm/:s and the ions at target center to be moving at velocities ≈ 2 cm/:s. As the target plasma expands there will be continued cooling of the electrons (the ions will be cold) and the electron density will continue to decrease volumetrically to the local ion density.

As a first look, let's assume that the average n_e decreases with time as the change in the target volume given by

$$n_e(t) \approx n_e(t = \tau_{ch}) \text{ X } \{ \text{ Vol}(t = \vartheta_{ch})/ \text{ Vol}(t) \}$$

which is

$$n_e(t) \approx n_e(t = \vartheta_{ch}) \text{ X } \{\tau_{ch}^3 \, v_{outer}\}/\{t^3 \, (v_{outer}^3 - v_{inner}^3)\}$$

If we assume that T_e bottoms out around 0.5 eV and using $v_{outer} \approx 6$ cm/μs and $v_{inner} \approx 2$ cm/μs, for

$\lambda_D \approx 250$ microns, $t \approx 10$ μs and L ≈ 60 cm.

So at reasonable distances from the target, we should be able to have a reasonable size pinhole (of order 250 microns) that should provide separation of the electrons from the ions internal to the ion charge state detector system.

Conclusions

So we can make some general conclusions on the expected plasma conditions. If the laser heating occurs on timescales of sub-100 picoseconds, we would expect the target material to be in quasi-LTE due to the high e-e collision rate and the early short e-i thermalization times. However, even for small targets with the assumed uniform T_e and n_e, in timescales less than the time for the target to expand (< few ns), the plasma T_e ,n_e and Z will have significantly decreased. The plasma material at the exterior of the target will expand at velocities characteristic of the initial T_e and with a relatively high degree of ionization. A rarification wave will propagate into the hot material at the ion sound speed and as the rarification wave propagates, then at the sonic interface, the interior hot material will then expand out at the expansion velocity determined by the local plasma ion temperature. Thus, the target material does not all expand at a uniform velocity, or temperature, or ionization state due to the rapid change in T_e and recombination.

Thus, at our detector system, we would expect to see a distribution of plasma velocities arriving with the exterior material arriving at velocities characteristic of the initial temperature (highest velocities) and the interior material having lower velocities and ionization levels as determined by collisional and radiative process in the first few nanoseconds of the expansion. Also, we can expect that the charge state of the expanding plasma to be rapidly be 'frozen out' at charge states near to that at the beginning of their expansion. This can be seen as recombination rates go as the square and/or cube of the local electron density that is rapidly changing due to recombination but primarily decreasing by volumetric effects ($1/r^3$). Clearly, to have a better understanding of the target expansion phenomenon will require an accounting for the time dependent radiation losses, radiation transport, electron-ion collisions, and recombination and atomic emission. For the design of our experiment, then clearly a variable in the shot matrix is the target initial density, size and shape.

IV. Review of Trident Laser Xenon gasbag experiments

Of consideration for targets on the HELEN experimental SGEMP campaign are small xenon gas bags. It may be of value to review the results of experiments performed on a similar energy laser using xenon gas bags. The experiment measured the M-shell and L-shell emission at the Trident at LLNL with typical laser parameters of 0.5 TW at 2ω. Targets were Al cylinders

filled with 0.77 atm. of xenon, an LEH of 0.35 micron polyimide and a rear window of 6 micron Mylar (Figure 5). Assuming an effective ionization to the L-shell (45+), the electron density was 10^{21} e/cm^3 or 0.24 n_{crit} at 0.53 microns. The average laser intensity was 10^{15} W/cm^2 with a 460 ps laser pulse width. X-rays were measured with filtered diamond-PCD and Si-PIN detectors. The Xe spectrum from 4-6 keV was recorded with a crystal spectrometer. The efficiency and spectrum were compared to Ti discs shot under the same conditions as the xenon.

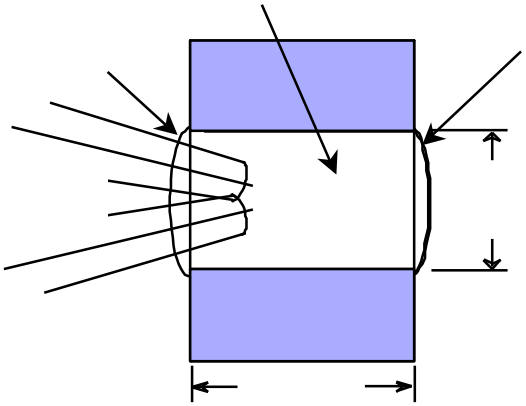

Figure 5: Schematic of xenon gasbag target used on the Trident laser

A series of calculations were performed pre-shot by Larry Suter of LLNL assuming 0.5 TW laser, a 0.5 ns pulsewidth, and a laser intensity of 10^{15} w/cm^2 onto 0.004 g/cm^2 xenon gasbag. His calculations predicted 77% laser absorption in gas, and 39% of the incident laser energy would be converted to x-rays. The calculated efficiency is 20% below 1 keV, 18% in M-shell between 1-3 keV and 1.16 % in L-shell > 4 keV. The experiments observed efficiency (photons out/laser energy to target) for the M-shell between 1-3 keV was 21.7% but only 0.56% in the L-shell above 4 keV.

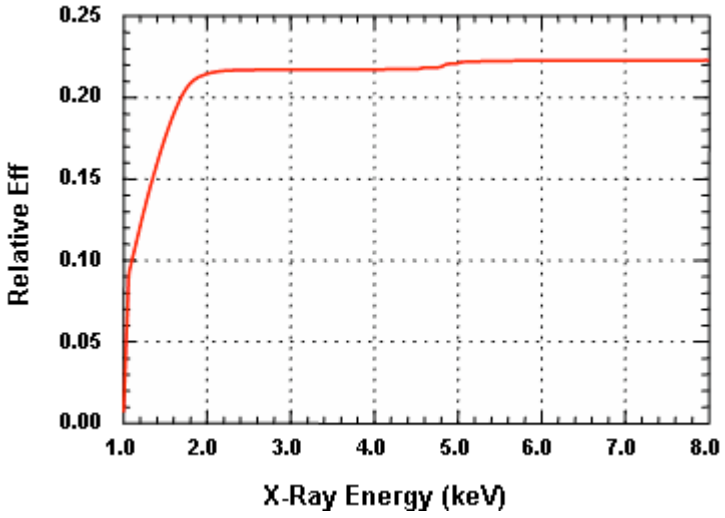

Figure 6: Experiment results of conversion efficiency of xenon gasbags on Trident.

V. HELEN Planning

In preparations for the HELEN Charge State Freeze Out (CSFO) and SGEMP experiments, estimates of the maximum expected signals were made and desired standoff of the detectors from the HELEN vacuum tank. An estimate of maximum signals was made with simple equation and simplifying assumptions

$$\text{Signal} = \{E_L \bullet f_{abs} \bullet CE/4BR^2\} \times \{\text{Target Geo}\} \times \{R_D \bullet A_D \bullet T_F \bullet T_s \bullet 50/\tau\}$$

f_{abs} = fraction of laser energy absorbed in target
R_D = detector response (amps/cm^2-MW)
A_D = area of the detector (or area of pinhole in front of detector)
T_F = transmission of filter (if used)
T_s = transmission of screen (if used)
τ = x-ray pulsewidth

CSFO

For the Charge State Freeze Out (CSFO) experiments, assume targets of SiO_2 with laser energy/power of 5-30 J, a pulsewidth of 0.5 psec, 60 TW. For the calculation it is assumed that the absorbed laser fraction f_{abs} is 100% and that the x-ray detectors can observe the full volume of emission, Target Geo ~ 1.0. For these experiments the expected radiation output will be a quasi-continuum with a characteristic blackbody temperature of 30-50 eV. Therefore most of the radiation will be in the photon range of ~60 – 200 eV. Further assume that the radiation output is in about 1 ns and the conversion efficiency of 40%. We plan to use detectors from IRD corporation that have excellent response in this photon range. The IRD, silicon detectors, response at 80eV is ~0.25×10^6 A/MW and the detectors are mounted in an SMA F/F brass bulkhead. The active area of the detector is 1x1 mm or 0.01 cm^2 and the typical bias is 50 V.

Thus, for R = 250 cm, Signal estimate (1st cut) ~ 2 kV

This is of course no good and since there are practical limits for the detector standoff, it is assumed to use a pinhole and nickel micromesh screens in front of the detector to reduce the flux (and signal). Assuming a 75 micron pinhole and a Ni micromesh screen with 7.62 micron holes, 78.7 holes/mm; $T_s = 0.36$

Signal estimate (2nd cut) ~ 3V

Which is OK. The addition of the pinhole requires extra caution in alignment of the detectors to the target. So, it is suggested that the IRD Silicon pindiodes be at least 250 cm from TCC (400 cm more desirable as will allow use of bigger pinhole). For the HELEN experiments they are planned to be on Port 24 which (I think) is 87 cm from TCC. One issue is mounting of our detector array to the HELEN vacuum tank and it needs to be decided who makes the flange to hold the pin diodes. I think that a standard Quick Flange 50 mm ID (QF50 blank flange) will work and we will need three-four SMA vacuum bulkheads feedthroughs mounted through it on about a 25mm diameter circle.

SGEMP

For the SGEMP experiments, it is desired to have x-ray emission in the multi-keV range. The proposed primary sources for the experiments are xenon gasbags with output from the M-shell of 0.8-3 keV and the L-shell around 4-6 keV. For estimates of the expected signal it will be assumed that both the East & West main beams of the laser will be used with 350 J each, and a typical pulsewidth of 1 nanosecond. The targets will be xenon gasbags, TiO_2 foam, and Ti disks.

For the calculation it is assumed that the absorbed laser fraction f_{abs} is 100% and that the x-ray detectors can observe only about ½ of target volume of emission, Target Geo ~ 0.5. For our standard XRDs, the area of the detectors are $A_D = 0.32$ cm^2 and to reduce noise and to protect the filters a Be filter ~12.5 microns thick will be used. This will limit the observed photons to energies above about 1 keV and the Be filter is only ~ 30% transmission at 1.1 keV. As discussed in the review of the xenon gasbag experiments on the Trident laser, the HELEN laser conditions will be very similar, and thus we would expect most of radiation out to be 800-1200 eV. It is therefore reasonable to assume that the x-ray output is about 1 ns and that the conversion efficiency above 1 keV of 20%. For a lower energy channel XRD (more sensitive channel), the average responsivity will be about 10 A/MW. The XRDs are mounted in on a QF50 flange and are planned to be on Port 38 which is 100 cm from TCC, so the XRDs with its current mount tube puts them at 117 cm from TCC.

Plugging into the equation for the signal at 117 cm: Signal ~ 20V which is marginal.

For R = 250 cm, Signal estimate (1st cut) ~ 4.3V ***-OK-***

So, the XRDs minimum distance would be 117 cm from TCC and it is suggested to mount them 250 cm, but anything more than around 150 cm should be OK.

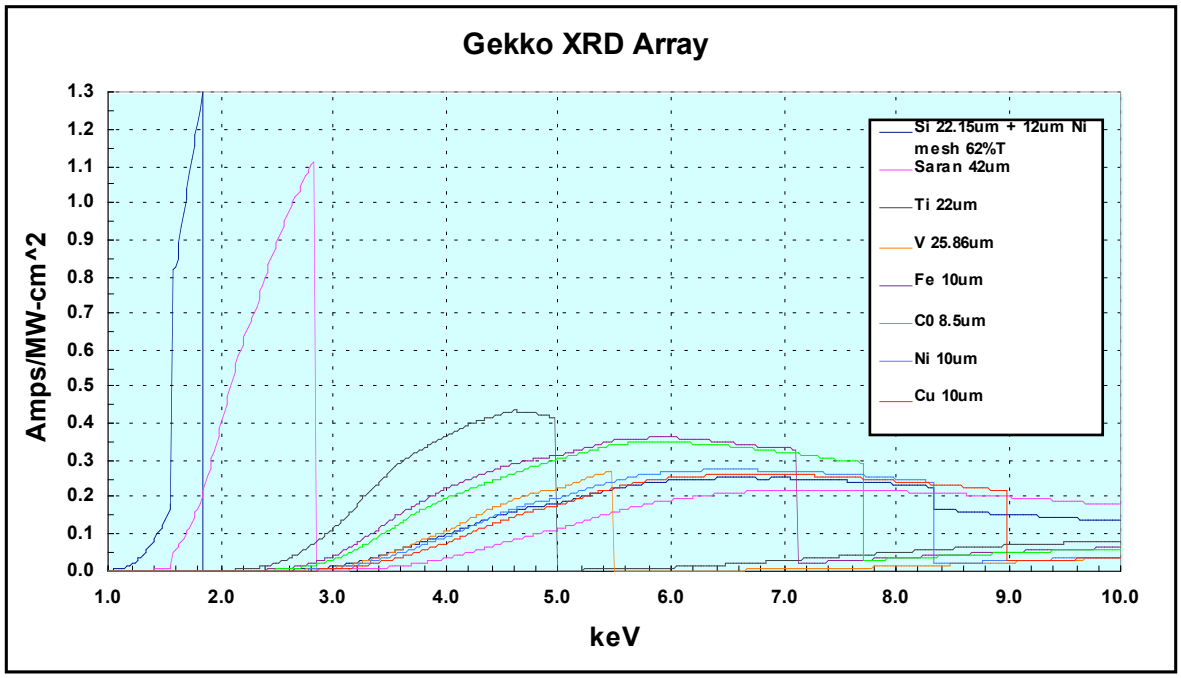

Figure 2: Response functions of the filtered XRD array used for the 2006 GEKKO XII campaign.

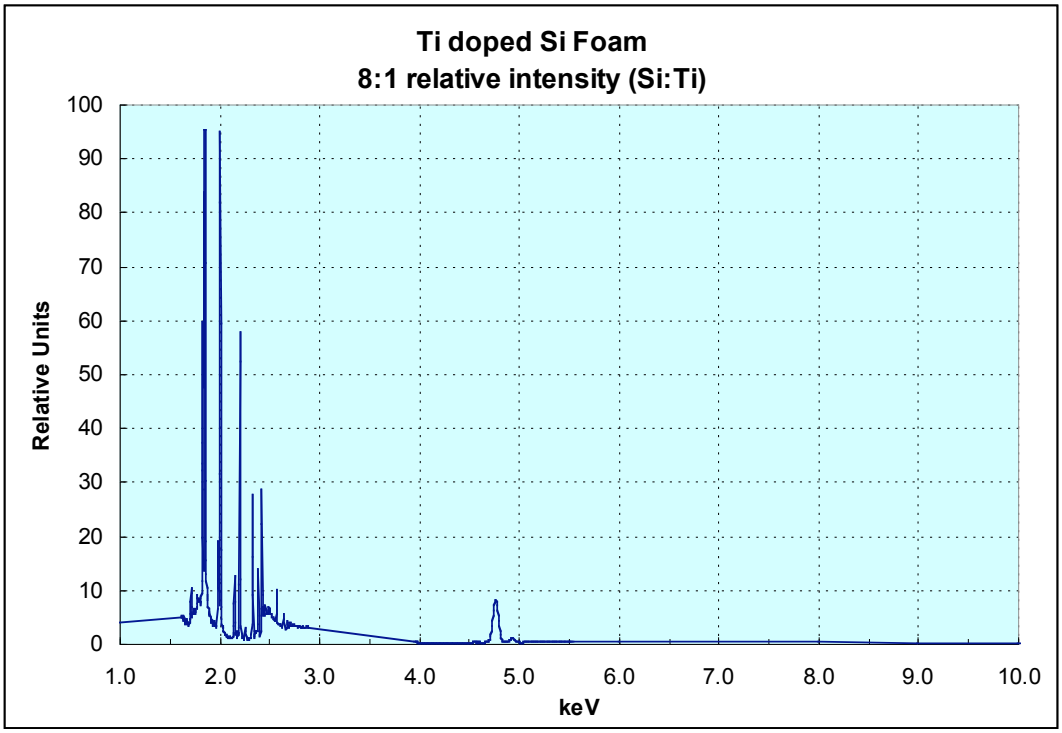

Figure 3: Sample start spectrum for Ti doped SiO_2 aerogel targets.